Metaheuristic Optimization of PI Control in Coupled Inductor SEPIC Converter for Photovoltaic Applications

[1]**Kavya Santhoshi B., [2]Parvathi R.V.L.N.S., [2]Tharpil H.G., [2]Vamsi K.M., [2]Appaji M. K.**

[1]School of Engineering, Godavari Global University, Rajahmundry, India
[2]Godavari Institute of Engineering and Technology (A), Rajahmundry, India

Abstract. Grid-connected PV systems remain essential to supply energy demands as the globe shifts its focus to renewable energy sources (RESs). Although there are many advantages to this integration, there are also a number of issues with power quality and stability at the connection points. The aim of the study is to tackle photovoltaic (PV) energy systems voltage instability poor dynamic response and to increase conversion efficiency in conventional control and converter configurations. The main objectives of the study were achieved by solving the following problems: (i) improving the DC-DC stage's voltage conversion capabilities, (ii) delivering stable DC-link voltage regulation under varied irradiance conditions, and (iii) optimizing the control system's dynamic and steady-state performance. To address these challenges, an intelligent power conversion system has been developed by combining a novel coupled inductor SEPIC (CIS) converter with an Osprey optimized algorithm-based proportional-integral (OOA-PI) controller. The most important result is that the proposed CIS-SEPIC converter and an OOA-PI Controller ensure to step up DC voltage output from the PV array while maintaining voltage stability. This controlled regulated DC output is supplied for a three-phase voltage source inverter (3φ -VSI) that transforms the DC power into AC power suitable for driving the connected load. The significance of the obtained results lies in improving the quality of electrical energy and reducing its losses. The system has been designed and tested using MATLAB/Simulink, offering better voltage regulation, faster transient response with low harmonic distortion AC output, and improved converter efficiency of 96% compared to the conventional method.

Keywords: photovoltaic, coupled inductor SEPIC converter, Osprey optimization algorithm, proportional-integral, three-phase voltage source inverter.

Optimizare metaeuristică a controlului PI în convertorul SEPIC cu inductoare cuplate pentru aplicații fotovoltaice
[1]**Kavya Santhoși B.[1], [2]Parvathi R.V.L.N.S. [2], Tharpil H.G., [2]Vamsi K.M., [2]Appaji M. K.**
[1]Școala de Inginerie, Universitatea Globală Godavari, Rajahmundry, India
[2]Institutul de Inginerie și Tehnologie Godavari (A), Rajahmundry, India

Rezumat. Sistemele fotovoltaice conectate la rețea rămân esențiale pentru satisfacerea cererii de energie, pe măsură ce lumea își îndreaptă atenția către sursele regenerabile de energie (SRE). Deși această integrare prezintă numeroase avantaje, există și o serie de probleme legate de calitatea și stabilitatea energiei electrice la punctele de conectare. Scopul principal al studiului este de a aborda provocările sistemelor de energie fotovoltaică (PV), inclusiv instabilitatea tensiunii, răspunsul dinamic slab și eficiența redusă a conversiei în configurațiile convenționale de control și convertizoare. Aceste obiective au fost atinse prin integrarea unui sistem inteligent de conversie a energiei, utilizând un convertizor SEPIC cu inductor cuplat (CIS) și un controler proporțional-integral (OOA-PI) bazat pe algoritmul optimizat Vultur pescar (Osprey). Cele mai importante rezultate constă în faptul ce convertorul CIS propus permite creșterea tensiunii de ieșire de curent constant (CC) din panoul fotovoltaic, menținând în același timp stabilitatea tensiunii. OOA folosit reglează în mod optim parametrii controlerului PI, asigurând o tensiune DC-link controlată cu precizie, reducând eroarea în stare staționară și îmbunătățind semnificativ răspunsul dinamic. Această ieșire CC controlată și reglată este furnizată unui invertor trifazic cu sursă de tensiune (VSI) care transformă energia CC în energie CA adecvată pentru alimentarea sarcinii conectate.

Semnificația rezultatelor obținute constă în demonstrarea faptului că sistemul a fost proiectat și testat utilizând MATLAB/Simulink, oferind o mai bună reglare a tensiunii, un raspuns tranzitoriu mai rapid cu o distorsune armonică redusă a ieșirii de current alternativ.

Cuvinte-cheie: fotovoltaic, convertor SEPIC cu inductor cuplat, algoritm de optimizare Osprey, invertor de tensiune trifazată, proporțional-integral.

Метаэвристическая оптимизация ПИ-регулятора в преобразователе тока с сопряженным индуктором для фотоэлектрических приложений

[1]Кавья Сантоши Б., [2]Парвати Р.В.Л.Н.С. [2], Тарпил Х.Г., [2]Вамси К.М., [2]Аппажи М.К.

[1] Глобальный университет Годавари, Раджамандри, Индия.

[2]Инженерно-технологический институт Годавари (A), Раджамандри. Индия

Аннотация. Подключенные к сети фотоэлектрические системы, по-прежнему, играют важную роль в обеспечении энергетических потребностей, поскольку мир все больше ориентируется на возобновляемые источники энергии (ВИЭ). Несмотря на многочисленные преимущества такой интеграции, существует ряд проблем, связанных с качеством и стабильностью электроэнергии в точках подключения. Основная цель исследования — решить проблемы фотоэлектрических (PV) энергетических систем, включая нестабильность напряжения, плохую динамическую реакцию и низкую эффективность преобразования в традиционных конфигурациях управления и преобразователей. Эти цели были достигнуты за счет интеграции интеллектуальной системы преобразования энергии с использованием нового преобразователя напряжения со связанным индуктором (ПНСИ) и ПИ – контроллера, оптимизированного по методу Скопы. Наиболее важными результатами являются то, что предлагаемый преобразователь ПНСИ позволяет повысить выходной постоянный ток от фотоэлектрической батареи, сохраняя стабильность напряжения. Используемый алгоритм оптимизации оптимально настраивает параметры ПИ-контроллера, обеспечивая точное управление напряжением в цепи постоянного тока, уменьшая постоянную погрешность и значительно улучшая динамическую реакцию. Этот регулируемый выход постоянного тока подается на трехфазный инвертор напряжения, который преобразует постоянный ток в переменный, подходящий для питания подключенной нагрузки. Значение полученных результатов заключается в том, что система была разработана и протестирована с использованием MATLAB/Simulink, что обеспечивает лучшую регулировку напряжения, более быструю переходную характеристику с низким уровнем гармонических искажений переменного тока.

Ключевые слова: фотоэлектрические системы, преобразователь ПНСИ со связанным индуктором, алгоритм оптимизации Оспри, пропорционально-интегральный преобразователь, трехфазный инвертор напряжения.

I. INTRODUCTION

The increasing global energy demand, along with the diminishing of conventional energy derivatives and their harmful environmental effects, is pushing the world towards a potential energy crisis within the next few decades. The burning of fossil fuels emits NO, CO_2, and NO_2 gases which greatly contributes to global warming and environmental pollution [1-2]. These challenges have hastened the global transition from fossil fuels to renewable energy sources (RES) for energy generation.

The amount of renewable energy systems installed around the world is accelerating rapidly due to the potential for reducing greenhouse gas emissions, air quality improvement, and energy security [3].

Among the various RES solar energy considered as the most viable option, due to its abundant availability, cleanliness, zero emission and ecological friendly [4].

PV systems convert solar radiation into electricity directly and play a significant role in sustainability development in energy [5].

However, the power output of PV system is inherently variable, primarily driven by the factors such as solar radiation, temperature, etc. To ensure that PV systems deliver stable and usable voltage levels, the low fluctuating DC output from solar modules need to be stepped up, a DC-DC converters is essential [6-7].

Various existing converters are developed in the previous studies as shown in Table1. In addition, when controlling these converters, PI controller are typically used for their ease of implementation, low cost and consistent performance that minimizes steady-state error and oscillations in the system response [8].

However, a PI controller requires proper tuning of its parameters, and there is a risk of poor dynamic response or system instability if improperly tuned. Therefore, optimization methods applied to find optimal PI gains that allow for reliable system operation that yields improved power regulation under changing environmental factors [9-10]. Table 2 illustrates the existing study of optimized PI controllers.

Table 1

Literature survey of existing converter.

Author / Year	Converter	Pros & Cons
Nafis Subhani *et al* (2023) [11]	Improved Quadratic Boost converter (IQB)	**Pros:** Lower voltage stress on semiconductor switch, diodes and capacitor. Uninterrupted source current and common ground features
		Cons: The dual-switch configuration necessitates the use of two separate control power supply. Increasing system costs for budget applications.
Omar Abdel-Rahim *et al* (2020) [12]	High Step-Up DC-DC converter (HSUDC)	**Pros:** This converter boost up the input voltage, which impressive for higher powering voltage system from PV modules.
		Cons: Operating at high duty cycles and switching frequencies lead to increased switching losses, reducing efficiency.
Arshad Mahmood *et al* (2021) [13]	Non-Inverting High Gain DC-DC Boost converters (NIHGDCB)	**Pros:** Higher gain of voltage at lower duty cycle, involves minimal voltage stress on switch and diodes
		Cons: Efficiency drops at higher output power due to switching and conduction losses, Limited to medium power applications.
Shahrukh Khan *et al* (2021) [14]	Ultra High Gain DC-DC Boost converter (UHGDCB)	**Pros:** It uses switched inductor and capacitor to boost voltage without transformer, Low voltage stress.
		Cons: Efficiency degrades at very low input due to conduction loss.
Harish Chandra Mohanta *et al* (2022) [15]	SEPIC Converter	**Pros:** Supports step up and step down modes, Maintain continuous input current and suitable for wide rage PV voltage
		Cons: High control complexity and reduced efficiency at high duty cycles.

Table 2

Literature survey of existing optimized PI controller.

Author / Year	Optimized PI Controller	Pros & Cons
M.F. Roslan *et al* (2020) [16]	Particle Swarm Optimization (PSO-PI)	**Pros**: this controller minimising voltage regulator error, improve performance of power quality, decrease DC link voltage oscillation, and reduction the harmonics.
		Cons: The absence of real-time hardware validation, limits the assessment of real-time performance and practical applicability.
D Sivamani *et al* (2021) [17]	Genetic Algorithm (GA-PI)	**Pros:** Significantly reduces steady-state error, Global search capability avoids local minima, enhanced dynamic responses.
		Cons: Requires significant computation time for optimal tuning, especially for large search spaces
G. Vasumathi *et al* (2023) [18]	Gray Wolf Optimization (GWO-PI)	**Pros:** Achieve global optimum without getting stuck in local minima, faster convergence with fewer iteration
		Cons: Real time implementation resource intensive depending on hardware and higher resource complexity.
Hazem Hassan Ellithy *et al* (2024) [19]	Marine Predator Algorithm (MPA-PI)	**Pros:** enhance steady state accuracy of the inverter output under grid fault conditions. It offer strong global search ability and fast convergence in optimization
		Cons: Validation is only simulation based; no hardware implementation is reported. Its structure make a computational burden in real time applications.
Nagwa F. Ibrahim *et al* (2023) [20]	Artificial Rabbit Optimization (ARO-PI)	**Pros:** Minimizes integral of squared error to obtain optimal PI controller, Maintain continuous operation in PV system during voltage sags and faults.
		Cons: ARO increases the computational burden during tuning.

Given the limitations of traditional converters and optimized PI controllers, this work proposes an OOA-PI controller integrated with a CIS converter for enhancing voltage regulation and system performance. The major contributions of this research include:

- PV system is used to create stand-alone DC power, which is converter solar energy into DC voltage.
- CIS converter is implemented to step up the low DC voltage into higher DC voltage present at the PV source.
- An OOA-PI controller is employed to control the converter, providing optimal parameters for improved response and reduced steady-state error.
- A 3φ-VSI is implemented to convert the regulated DC voltage into AC to efficiently supply power to a load.

II. PROPOSED SYSTEM DESCRIPTION

The proposed system, illustrated as Fig. 1, effectively deliver an AC load using a PV source. The PV system deliver an unregulated DC output in an array of voltage V_{pv} and a current I_{pv}. The unregulated DC power supplied to the CIS converter, which synergistically steps up the low PV voltage to a higher DC voltage. Due to the relatively unstable voltage of the PV structure, a PI controller embedded within the CIS converter allow to control the output voltage. The PI controller tuned adaptively, using OOA, which dynamically adjusts the K_p and K_i gains to achieve optimal performance in the transient and steady state through irradiation and load changes.
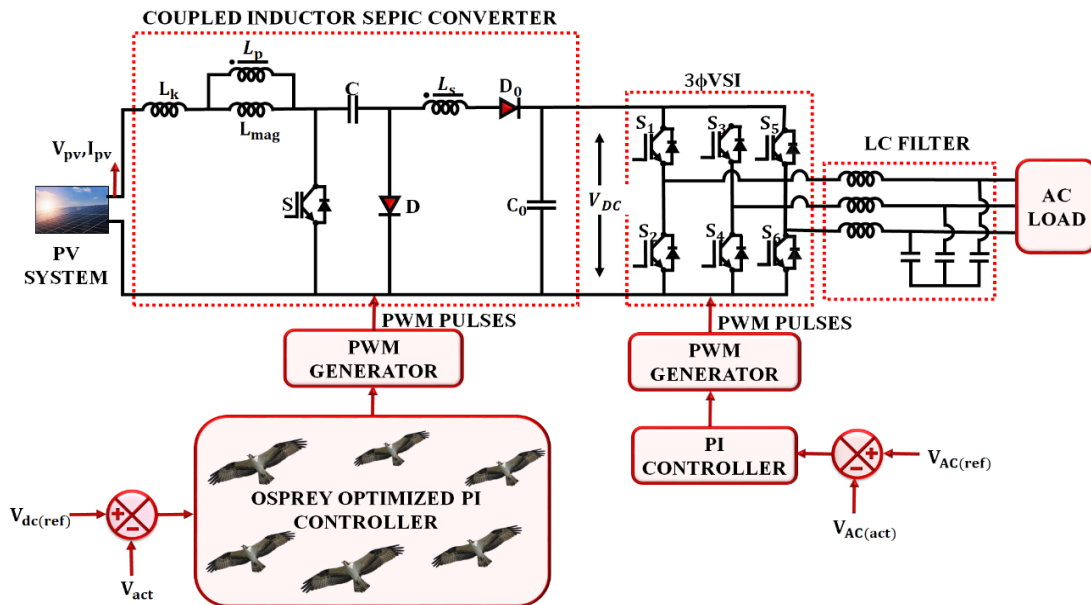
Fig. 1. Proposed block of PV system using CIS converter and OOA-PI controller.

The measured DC voltage output then supplied to a 3φ-VSI, which perform DC-AC transformation and output the necessary voltage indicated by the AC load. However, in order to keep the voltage stable and correct signal, a second PI controller is implemented in the inverter stage.

The hierarchical control system manages the power delivery system from a solar PV source, to supply the demand of AC loads while maintaining stability and performance of large fluctuations in solar input or load variations.

III. PROPOSED METHODOLOGY

A. PV System

A PV module contains of multiple solar cells linked in parallel and in series. The single-diode model in Fig. 2 includes a photo current source, a diode, and a series resistance, where all three elements of the model include temperature and irradiance effects. The photo current generated by sunlight is modeled using the source, while the diode serves in this model as a half-wave rectifier. The output current of the PV device, therefore, described bellow:

$$I_{PV} = I_{ph} - I_d \qquad (1)$$

Here, I_{PV}, I_{ph} and I_d denotes PV current, photocurrent, and diode current. The Shockley equation, which written as follow, is used to determine the diode current I_d :

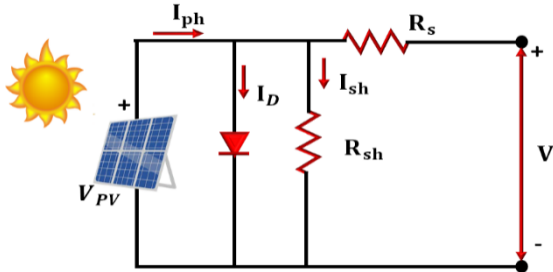$$I_d = I_S \left[exp\left(\frac{q(V_{PV} + I_{PV}R_s)}{\eta K_b T_k} \right) - 1 \right] \quad (2)$$

Fig. 2. Circuit diagram of PV model.

The PV cell output current is signified as below,

$$I_d = I_S \left[exp\left(\frac{q(V_{PV} + I_{PV}R_s)}{\eta K_b T_k} \right) - 1 \right] \quad (3)$$

Here, I_S and V_{PV} represents diode reverse saturation current and terminal voltage. R_s and R_p denotes series and parallel resistance. $\eta, K_b,$ and T_k stands ideality factor, Boltzmann constant and temperature of cell. Charge of electron denoted by q. Due to changes in irradiance and temperature, the PV system produces low and variable DC voltage. This requires a converter to increase the voltage for stable and efficient delivery, which is discussed below.

B. Coupled Inductor Sepic Converter

The CIS converter is a coupled inductor providing a greater voltage gain, lower input current ripple and higher efficiencies. The most important part of the converter in Fig. 3, contains leakage inductance L_k, primary winding L_p, magnetizing inductance L_{mag}, the secondary winding L_S as well as the series coupling capacitor C, the diode D and D_0, the output capacitance C_0 the load resistor, and a power switch S. The converter works by transferring energy from the input to output by stepping up or stepping down the input voltage, providing higher efficient connections.
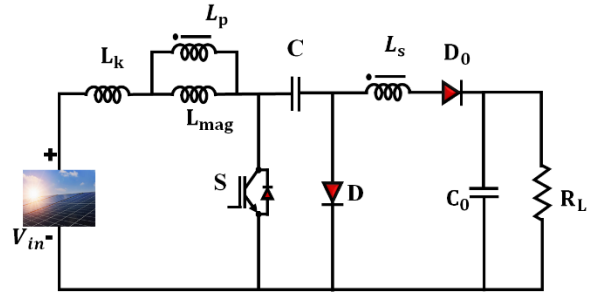

Fig. 3. Proposed CIS converter.

Mode 1: When switch S is ON and diode D_0 is reverse-biased as presented in Fig. 4 (a), the input voltage charges both leakage inductance L_k and magnetizing inductance L_{mag}. At the same time, capacitor C discharges the energy that it is storing into the load through diode D, and capacitor C_0 continues to provide current to the load powered continuously without interruption. During this period, the current travels from the input over the L_k and L_{mag}, then through the closed switch S, while a parallel path includes: current from capacitor C through diode D to load resistor R_L.

$$V_{Lk} = V_{in} \quad (4)$$

$$V_{Lmag} = V_{in} \quad (5)$$

Mode2: When switch S in the OFF position and diode D_0 conducting as presented in Fig. 4(b), the energy in magnetizing inductance L_{mag} and leakage inductance is released through the output. The energy does flow through the secondary winding L_s, coupling capacitor C, and diode D_0, while the input voltage goes directly to the output through the coupling winding. The path of energy during this stage begins at the input and discharging inductance through the secondary winding, before passing through capacitor C and diode D_0 and finally supplying power to load resistor R_L.

$$V_{Lk} = V_{in} - V_C \quad (6)$$

$$V_{Lmag} = -n \bullet V_C \quad (7)$$

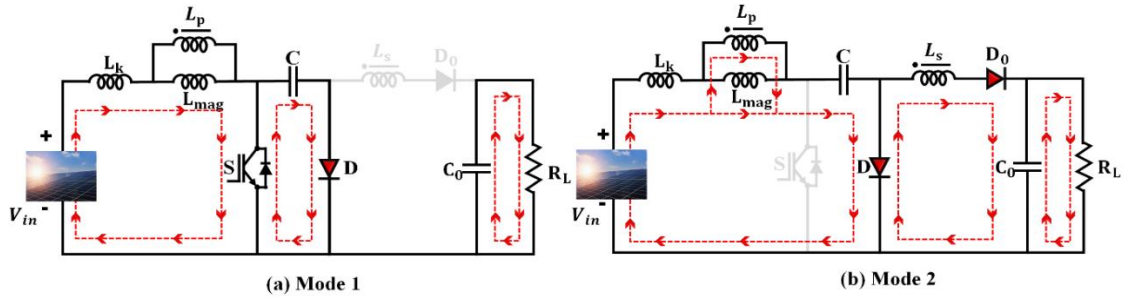When,

$$n = \frac{L_s}{L_p} \quad (8)$$

Fig. 4. Modes of operation (a) Mode 1 (b) Mode 2.

Using inductor voltage-current relations:

$$n = \frac{L_s}{L_p} \quad (9)$$

During Mode 1:

$$\frac{di_{L_k}}{dt} = \frac{V_{in}}{L_k} \quad (10)$$

$$\frac{di_{L_{mag}}}{dt} = \frac{V_{in}}{L_{mag}} \quad (11)$$

During Mode 2:

$$\frac{di_{L_{mag}}}{dt} = \frac{V_{in}}{L_{mag}} \quad (12)$$

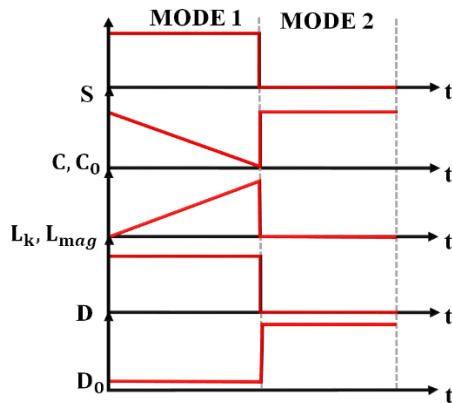$$\frac{di_{L_{mag}}}{dt} = -\frac{n - V_C}{L_{mag}} \quad (13)$$

Fig. 5. Switching waveform of proposed converter.

Applying volt-second balance over, L_k:

$$V_{L_k(on)} \cdot D + V_{L_k(off)} \cdot (1 - D) = 0 \quad (14)$$

$$V_{in} \cdot D + (V_{in} - V_C) \cdot (1 - D) = 0 \quad (15)$$

$$V_C = \frac{V_{in}}{1 - D} \quad (16)$$

Output voltage:

$$V_o = V_C + n \bullet V_C = V_C \bullet (1 + n) \quad (17)$$

$$V_o = \frac{V_{in} \bullet (1 + n)}{1 - D} \quad (18)$$

Figure 5 displays timing waveform of proposed converter, showing the gate signal, inductor voltage, and diode conduction periods. This converter attains a higher voltage gain and less switch and diode voltage stress and better efficiency by using coupled inductor and optimized energy transfer.

C. OSPREY optimized PI controller

The CIS Converter is controlled via a closed-loop feedback system with a PI controller, using the parameter's values which tuned from the proposed OOA. The PI controller has inherent problems such as peak overshoot and steady-state error. These problems are effectively reduced when the PI controller gains, such as proportional gain K_p and integral gain K_i are optimized using Osprey-based metaheuristic algorithm. The PI controller gains be described as:

$$u = k_p e + k_i \int_0^t e(\tau) d\tau = k_p (e + 1/T_i \int_0^t e(\tau) d\tau) \quad (19)$$

Here, k_p and k_i signifies proportional and internal gain constant, and $e(r)$ denotes error from real fixed point. Integral time constant denoted by T.
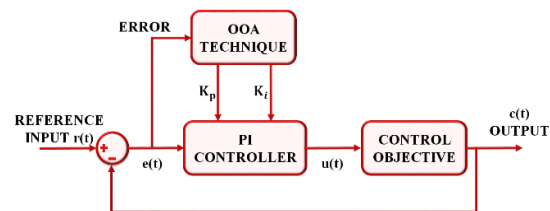

Fig. 6. PI controller diagram.

The conventional PI block illustrates in Fig. 6. Moreover, an optimization algorithm is incorporated in PI controller to determine selected gain values for optimum accuracy and stability.

Inspiration of OOA

The OOA resembles the intelligent hunting and prey-handling behavior of the osprey, known for its remarkable prey-targeting abilities with excellent vision in locating, tracking, and seizing its prey. The aim to model this natural ability of to locate, predict, and successfully seize has been fashioned into an optimization strategy. In this work, the intelligent foraging behavior of the osprey is modeled mathematically to develop the OOA, which is implemented to tune the PI controller gains, as illustrates in Fig. 7. This proposed algorithm mimics the decision making abilities of the osprey in an efficient manner of decision making with respect to targeting, while exhibiting improved control performance by reducing overshoot and steady state error in dynamic conditions.

Mathematical modelling

The mathematical modelling of proposed OOA is presented for the optimal tuning of PI controller gains K_p and K_i. The mathematical modelling consists of the initialization of the algorithm and processes of exploration and exploitation that find their foundations in natural osprey behavior.

Initialization

The OOA is a population-based metaheuristic algorithm in which individual ospreys, the animals, represent potential solutions, or a candidate set of PI controller gains K_p and K_i. The population of ospreys is randomly generated within the defined boundary for each gain parameter. Consequently, each osprey represents a candidate solution for problematic, which mathematically modeled with a vector. Ospreys collectively form OOA population and collectively model the ospreys using a matrix according to (20). At initialization of OOA, positions randomly in search space by using (21).

$$X = \begin{bmatrix} X_1 \\ \vdots \\ X_i \\ \vdots \\ X_N \end{bmatrix}_{N \times m} \begin{bmatrix} x_{1,1} & \cdots & x_{1,j} & \cdots & x_{1,m} \\ \vdots & \ddots & \vdots & \iddots & \vdots \\ x_{i,1} & \cdots & x_{i,j} & \cdots & x_{i,m} \\ \vdots & \iddots & \vdots & \ddots & \vdots \\ x_{N,1} & \cdots & x_{N,j} & \cdots & x_{N,m} \end{bmatrix}_{N \times m} \quad (20)$$

$$x_{i,j} = lb_j + r_{i,j} \cdot (ub_j - lb_j), i = 1, 2, \dots N; j = 1, 2, \dots, m \quad (21)$$

Here, X denotes population matrix signifies ospreys location, X_i denotes candidate solution $i-th$ osprey, and $x_{i,j}$ stands $j-th$ dimension.

N and m stands total amount of ospreys and problematic variables, $r_{i,j}$ stands random numbers in the range [0,1]. ub_j and lb_j denotes lower and upper bounds of $j-th$ problematic variable. These evaluated objective function values (F) used for tuning the PI controller parameters which are represented in the form of vector as below:

$$F = \begin{bmatrix} F_1 \\ \vdots \\ F_i \\ \vdots \\ F_N \end{bmatrix}_{N \times 1} = \begin{bmatrix} F(X_1) \\ \vdots \\ F(X_i) \\ \vdots \\ F(X_N) \end{bmatrix}_{N \times 1} \quad (22)$$

Here, F_i stands gained function value for $i-th$ osprey.

Phase 1: *Position estimation and prey search strategy (exploration)*

Phase 1 of OOA simulates the natural hunting behavior of ospreys. Ospreys are truly remarkable animals capable of using their extraordinary sense of vision to evaluate the location of fish deep underwater. Typically, an osprey skirts the area over a body of water, and upon spotting fish, dive and catch them. This behavior is replicated with OOA for tuning PI gains to account for major positional changes in the search space, allowing for more exploration by the algorithm and avoiding local optima. Each osprey has a set of the other ospreys with better objective values that impose as a fish target. Each fish set for $i-th$ osprey is defined as:

$$FP_i = \{X_k \mid k \epsilon \{1, 2, .., N\} \wedge F_k < F_i\} \cup \{X_{best}\} \quad (23)$$

Where FP_i signifies better solutions $i-th$ osprey, and X_{best} denotes best solution. The new position $x^P_{(i,j)} 1$ for each dimension j is calculated as:

$$x_{i,j}^{P1} = x_{i,j} + r_{i,j} \cdot (SF_{i,j} - I_{i,j} \cdot x_{i,j}) \quad (24)$$

$$x_{i,j}^{P1} = \begin{cases} x_{i,j}^{P1}, lb_j \le x_{i,j}^{P1} \le ub_j; \\ lb_j, x_{i,j}^{P1} < lb_j; \\ ub_j, x_{i,j}^{P1} > ub_j. \end{cases} \quad (25)$$

$$X_i = \begin{cases} X_i^{P1}, F_i^{P1} < F_i; \\ X_i, else, \end{cases} \quad (26)$$

Here $x_{i,j}^{P1}$ represents new position of $i-th$ osprey $j-th$ dimension, the objective function

value denoted by F_i^{P1}. $SF_{i,j}$ denotes selected fish for $i-th$ osprey $j-th$ dimension, $r_{i,j}$ stands random numbers in the range [0,1].
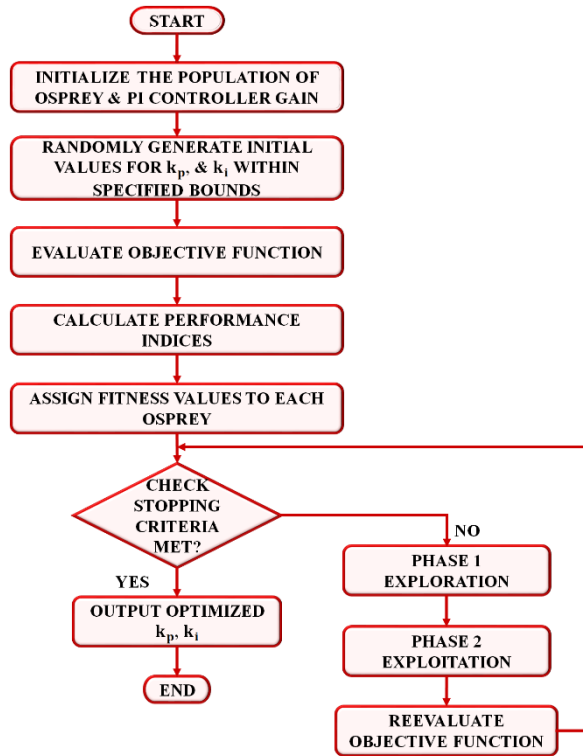

Fig. 7. Flowchart of OOA-PI controller.

Phase 2: Carrying the fish to the suitable position (exploitation)

In second phase of OOA [23], the osprey acts like carrying the identified safe location, local movement that increases the capacity for exploitation within the algorithm by allowing the algorithm to fine-tune the $(K_P \text{ and } K_I)$ parameters of PI around better solutions. For every candidate solution (osprey), a new position is randomly generated within the predefined boundaries. This new suitable position is evaluated to the objective function. If the new suitable position produces better controller performance (reduction in overshoot, reduced settling time, etc.) then the old gains $\left(K_P \text{ and } K_I\right)$ are replaced by the new suitable position gains.

$$x_{i,j}^{P2} = x_{i,j} + \frac{lb_j + r \cdot \left(ub_j - lb_j\right)}{t} \qquad (27)$$

$$\boldsymbol{x_{i,j}^{P2}} = \begin{cases} x_{i,j}^{P2}, lb_j \leq x_{i,j}^{P2} \leq ub_j; \\ lb_j, x_{i,j}^{P2} < lb_j; \\ ub_j, x_{i,j}^{P2} > ub_j. \end{cases} \qquad (28)$$

Table 3 signifies parameter specification of PV system and proposed converter.

$$X_i = \begin{cases} X_i^{P2}, F_i^{P2} < F_i; \\ X_i, else, \end{cases} \qquad (29)$$

Here $x_{i,j}^{P2}$ denotes new position of $i-th$ osprey $j-th$ dimension, the objective function value represented by F_i^{P2}. The OOA-PI controller to adaptively tune the control parameters of the converter to regulate the PV generated DC voltage precisely. The optimized and stable DC output is fed into a VSI and converted to a high-quality AC supply to the load. The output of the inverter then feeds into an LC filter capable of reducing high-frequency switching harmonics, thus generating a smooth sinusoidal waveform to supply the connected AC load. The system ensure continuous, reliable power transmission from PV source to the load in dynamic environmental conditions.

IV. RESULT AND DISCUSSION

In this work, a CIS converter with an OOA-PI controller is developed to effectively harvest PV energy and supply it to an AC load.

The developed system is modeled in MATLAB and evaluated constant condition and varying condition to assess its overall performance.

Under constant input, the output power remains stable, making it difficult to examine the converter dynamic performance, thus utilizing varying input, the converter response and control efficacy explicitly demonstrate and validated.

Table 3

Parameter Specifications.

| Parameters	Specifications
PV system	
Open Circuit Voltage	37.25V
Short Circuit Voltage	8.95V
Series Connected PV sell	17
Parallel Connected PV sell	4
Maximum Power Voltage	29.95V
Rated Power	15kW
CIS converter	
Switching Frequency	10KHz
L_p & L_s	4.7mH
L_k & L_{mag}	45mH
C	22μF
C_0	2200μF

**Condition 1:** Constant temperature and intensity.
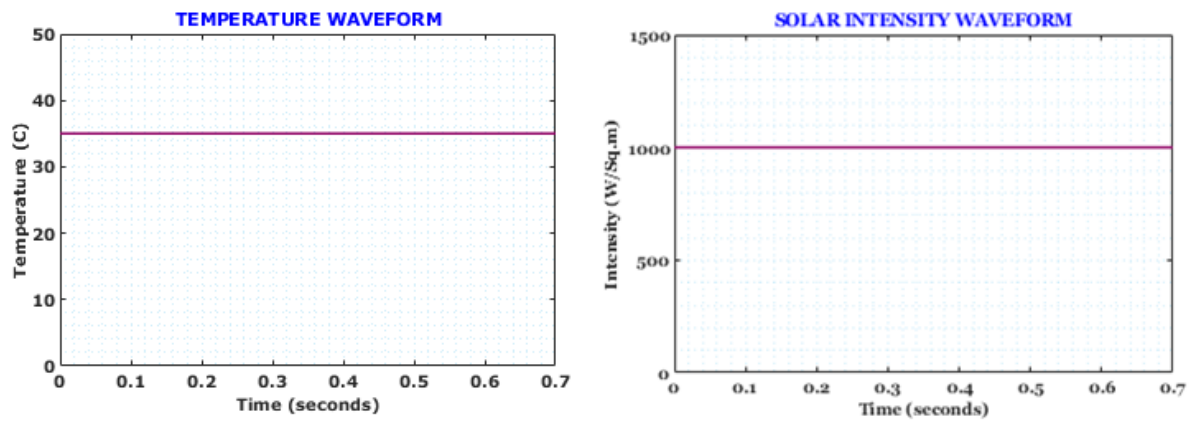
Fig. 8. Solar panel waveform under condition 1.

Figure 8 displays PV panel temperature and intensity under condition 1. The temperature constant at $35°C$, and solar intensity continue the constant at $1000W/m²$ through the simulation time. In this constant conditions, the PV output is constant, which delivers with a clear observation of the converter's behavior, where validate the effectiveness of the control strategy without interference from external variables.
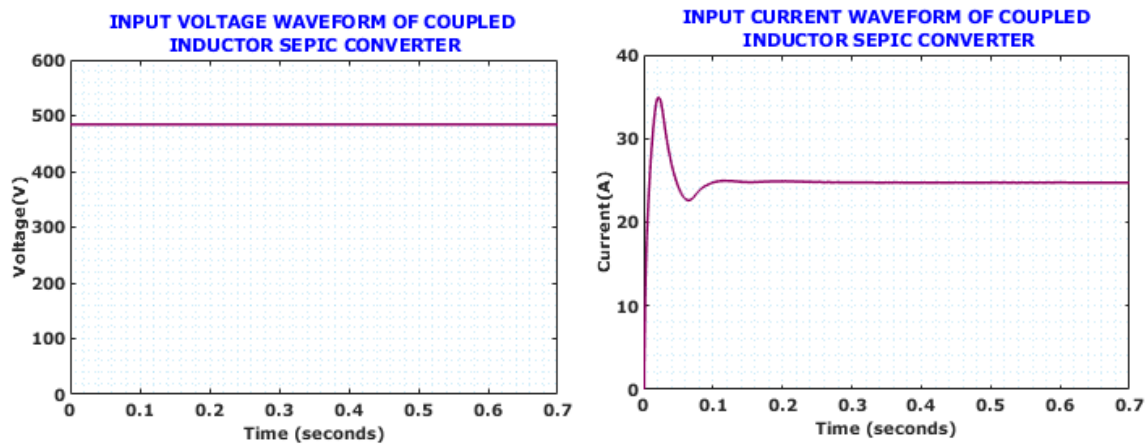
Fig. 9. Output waveform of PV panel under condition 1.
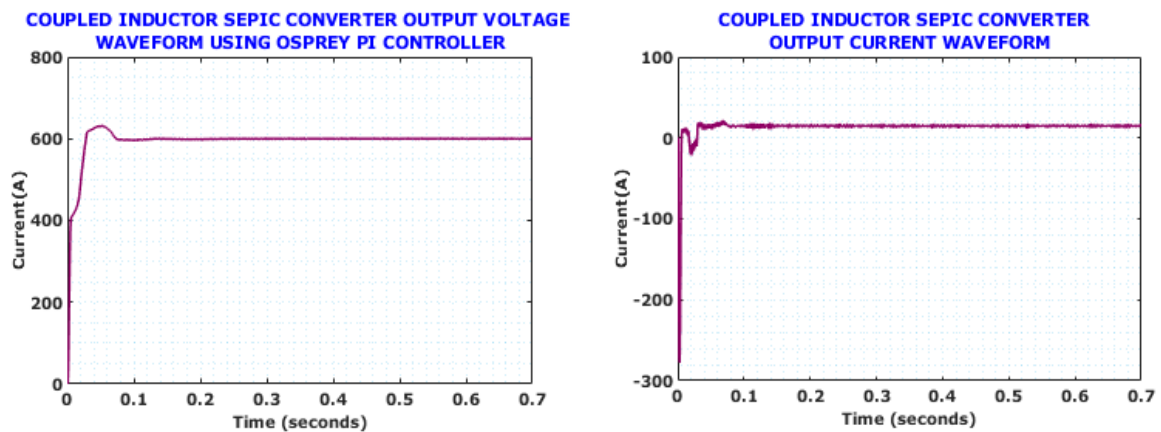
Fig. 10. Output waveform of converter under condition 1.

Figure 9 shows waveforms for the PV panel output under condition 1; there is the output voltage waveform which is constant at $500V$ showing a stable DC input from the PV array, with the input current waveform smoothly settling to a steady-state value of $25A$, presenting stable controlled input. The stability of the input current is primarily due to the constant PV conditions, and the natural settling of the converter after the initial transitory response.
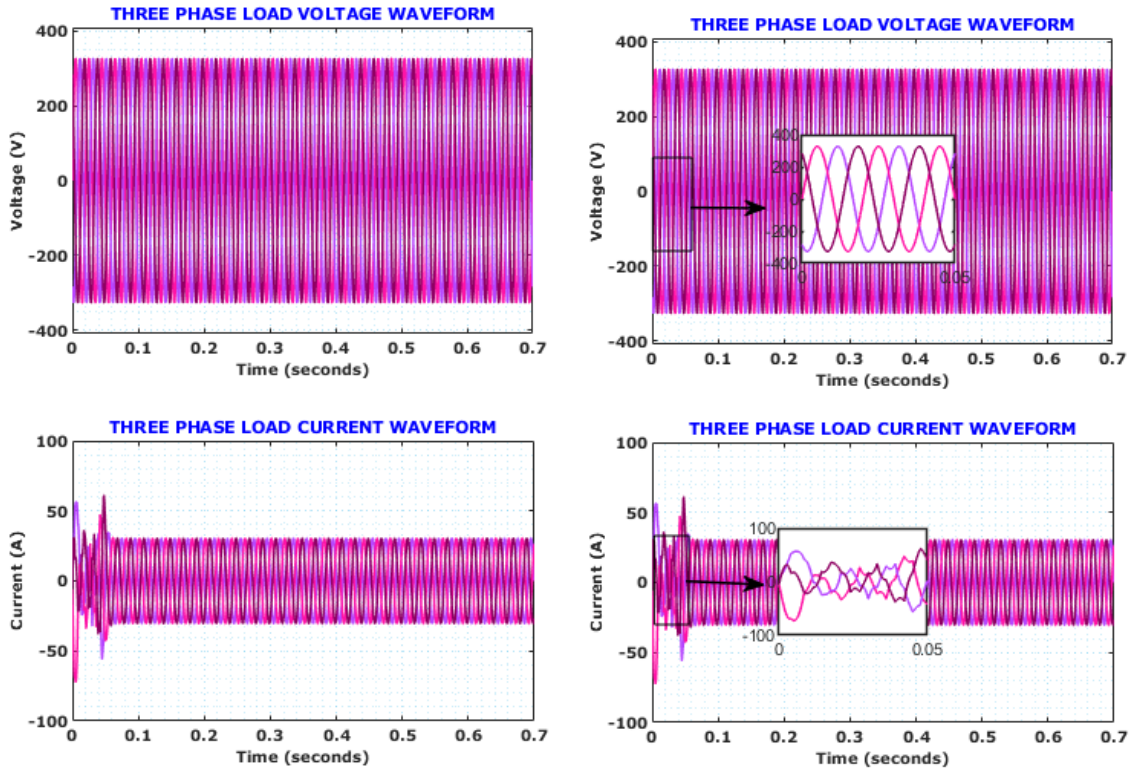

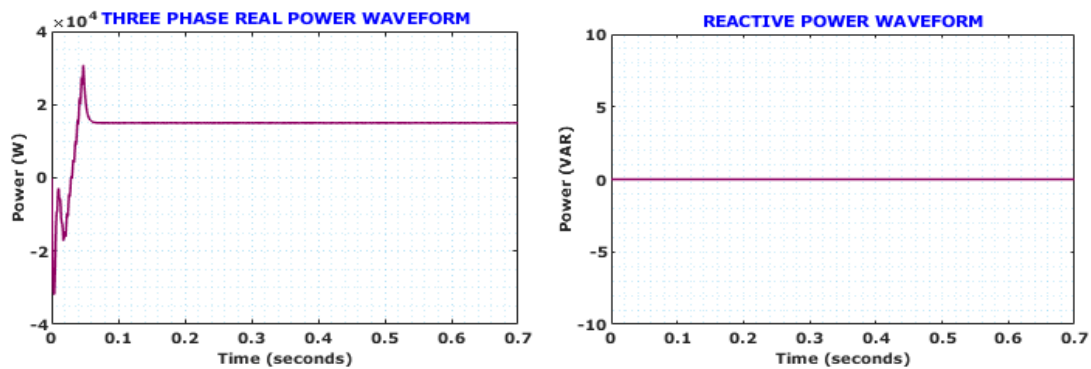**Fig. 11. Three phase load waveforms under condition 1.**

Fig. 12. Real and Reactive power waveform.

The converter's output performance under condition 1 is displayed in Fig. 10. Output voltage rise quickly and stabilize at $600V$, which illustrates voltage gain of the converter is achieved. Output current rises up to $20A$ settling to a steady value smoothly. Both voltage and current waveforms show a slight ripple and fluctuations due to start-up condition at the beginning, however due to the use of the OOA-PI controller, the transients are minimized quickly,

and the converter and inverter reaches steady-state rapidly.

Figure 11 shows the AC load waveforms under condition 1. The 3φ load voltage waveform shows balanced sinusoidal output voltage ranging at $\pm350V$, settling the inverter operating as expected. The load current waveform initially has small disturbances, but quickly settles and continuously deliver clean sinusoidal current at $\pm20A$.

Real and Reactive power waveform under condition 1 displayed in Fig. 12. The real power waveform during the simulation observed to rise up suddenly at the beginning, and to activate to nominally level out confirming stable active power supplied to the load. Reactive power waveform notably remains to zero for the duration of the simulation, signifying that almost all of the power transferred is real and able to be delivered to the load. This result demonstrates respectable conditions for energy conversion from PV source to AC load and is aligned with the goal of reliable and quality power delivery.

Condition 2. Temperature and Intensity Variations
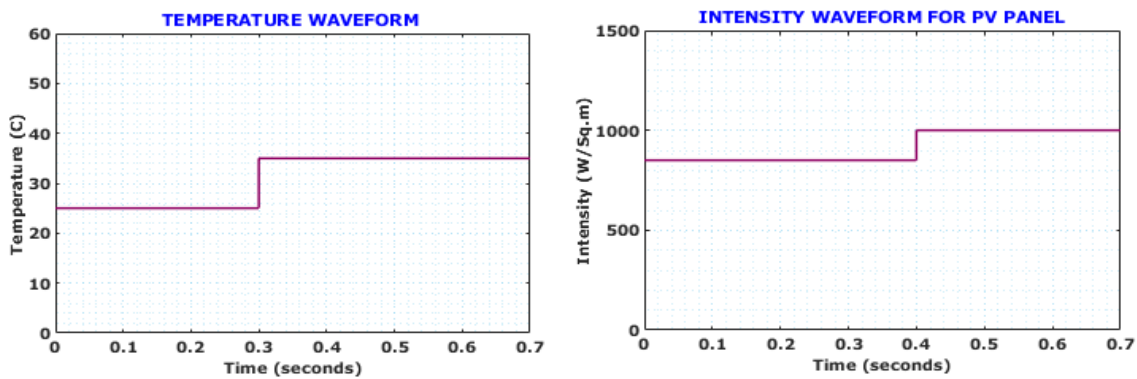
Fig. 13. Solar panel waveform under condition 2.

Figure 13 shows the varying temparature and intensity wavefoem under condition 2. The PV temperature increasing from $25°C\,to\,30°C$ at 0.3 s and irradiance rising from $800W/m²\,to\,1000W/m²$ at 0.4 s. These variations emulate realistic changes in environmental conditions, which is leads to the PV output voltage and current fluctuate, creating a dynamic input scenario for the converter.
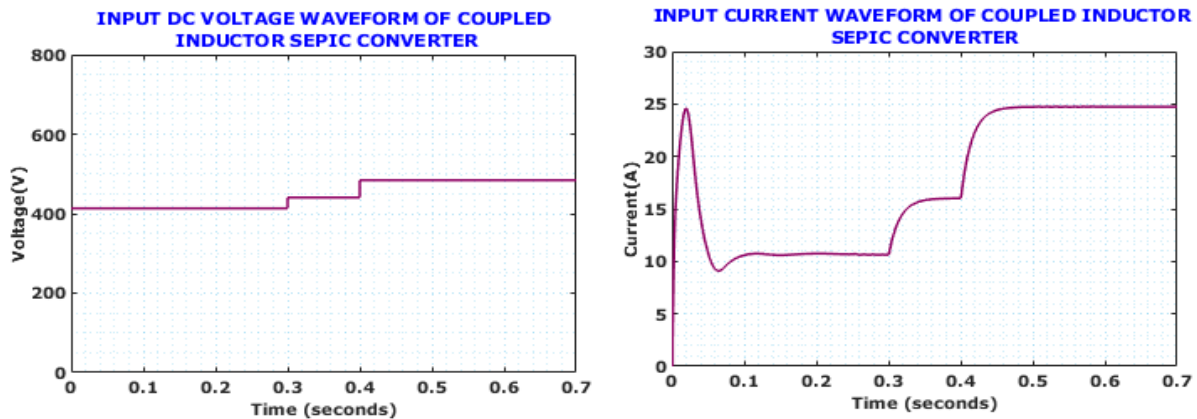
Fig. 14. Input waveform of proposed converter under condition 2.

Figure 14 shows the input waveform of PV panel under changing condition 2. The input voltage starts at $380V$ and rises at $500V$ after the irradiance is increased. The input current begins to rise and fluctuate and eventually settles after around 0.4 s at $21A$ as more irradiance increases the power output of PV. These signals show the PV response to changing weather conditions, indicating the converter need to operate over a wide range.
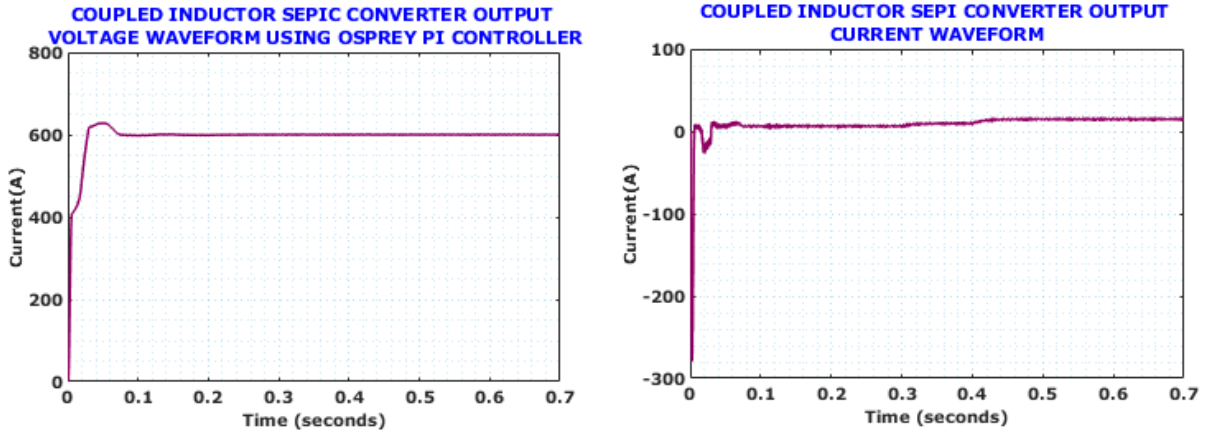
Fig. 15. Output waveform of converter under condition 2.

Converter output waveforms under condition 2 as displayed in Fig. 15. Even with variable input, the output quickly steadies at $600V$, and output current stabilizes at $20A$ with minimal ripple. This settles the OOA-PI controller quickly alter the duty cycle to regulate DC output voltage, even when PV conditions change.
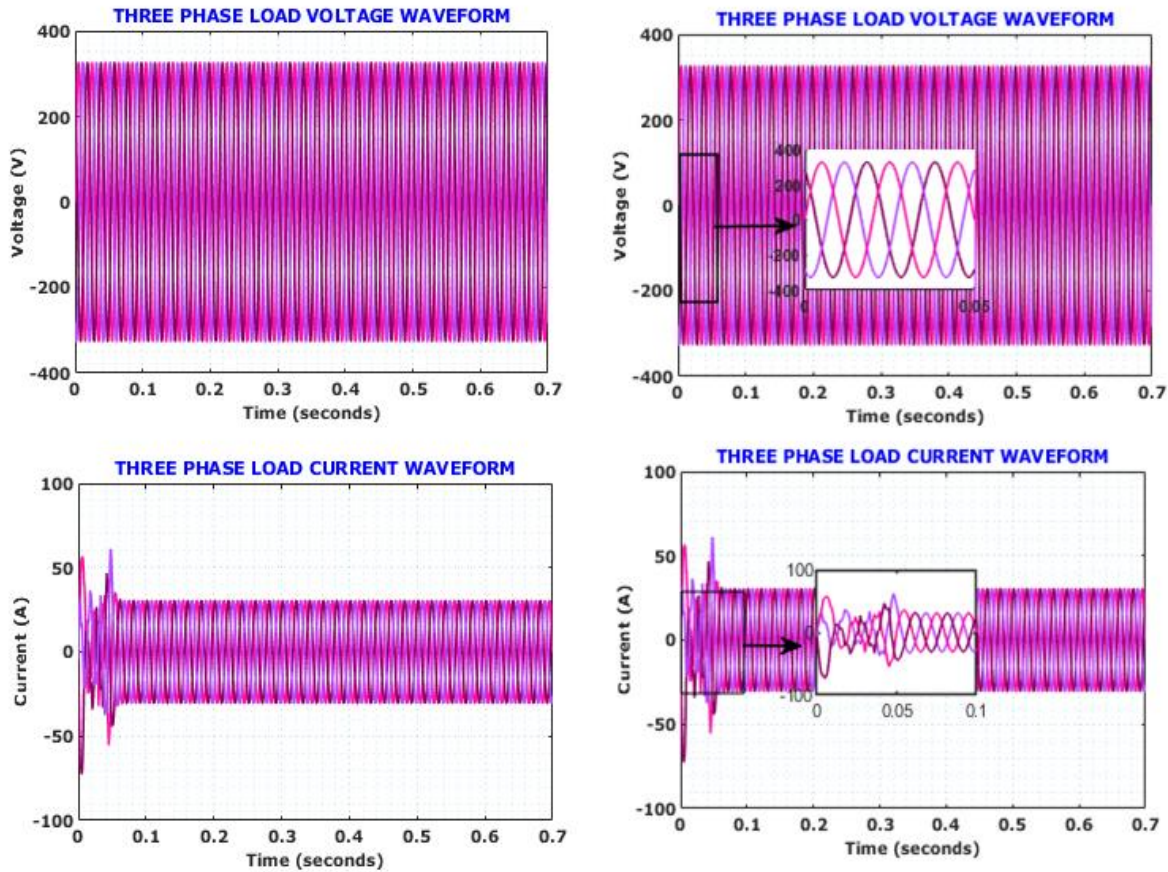
Fig. 16. Three phase load waveforms under condition 2.

The 3φ load waveform under condition 2 is presented in Fig. 16. The inverter continues producing balanced 3φ sinusoidal voltage ranging at $\pm400V$. The load current has a clean sinusoidal profile, indicating that the system is continuously supplying the load with high quality AC power regardless of the input varying conditions; this means that the load variation conditions doesn't affect the effectiveness of the converter and inverter.
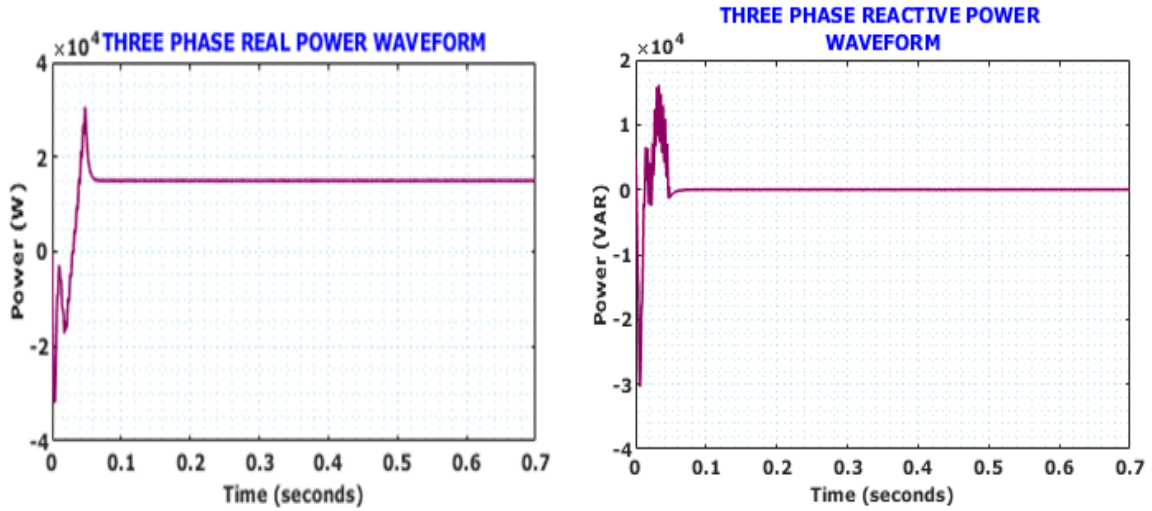
195

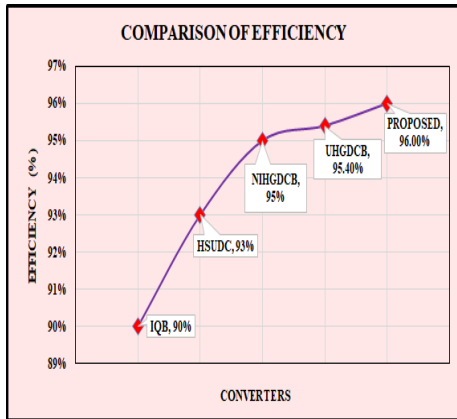**Fig. 17. Real and Reactive power waveform.**

Comparison:

Fig. 18. Evaluation of efficiency.

The results confirm that the varying temperature and irradiance conditions inherent in the experiment have been proven not to affect the performance of the system, as the converter and optimal controller performed as intended for providing efficient and reliable PV-to-AC power to the load regardless of the irradiance.

Figure 18 shows a comparison of efficiencies (%) among several converters, where the IQB converter [11] has 90%, HSUDC converter [12] has 93%, NIHGDCB converter [13] has 95%, UHGDCB converter [14] has 95.40%, and the proposed converter has a maximum efficiency of 96%. The proposed converter convert more input power to useful output power with minimal power loss resulting in better energy utilization, less heat, higher reliability of the system, and lower operating costs.
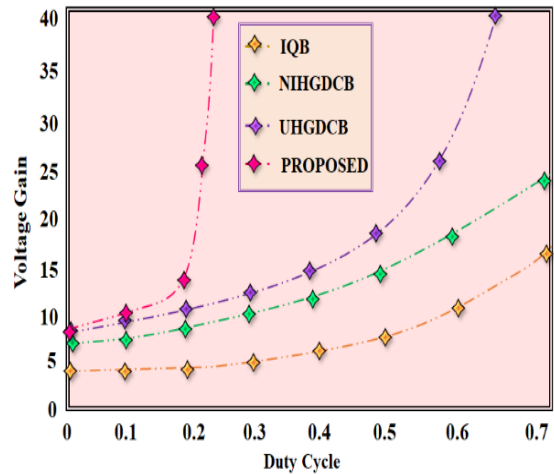

Fig. 19. Evaluation of Voltage Gain.

Real and reactive power waveform under condition 2 is shown in Fig. 17. The real power increases in direct proportion to the irradiance, and ultimately settles into a steady value that corresponds to the higher energy input from the PV array. While this occurs, the reactive power remains near zero, indicating a better power factor, significance that most of the supplied power is effectively used by the load.
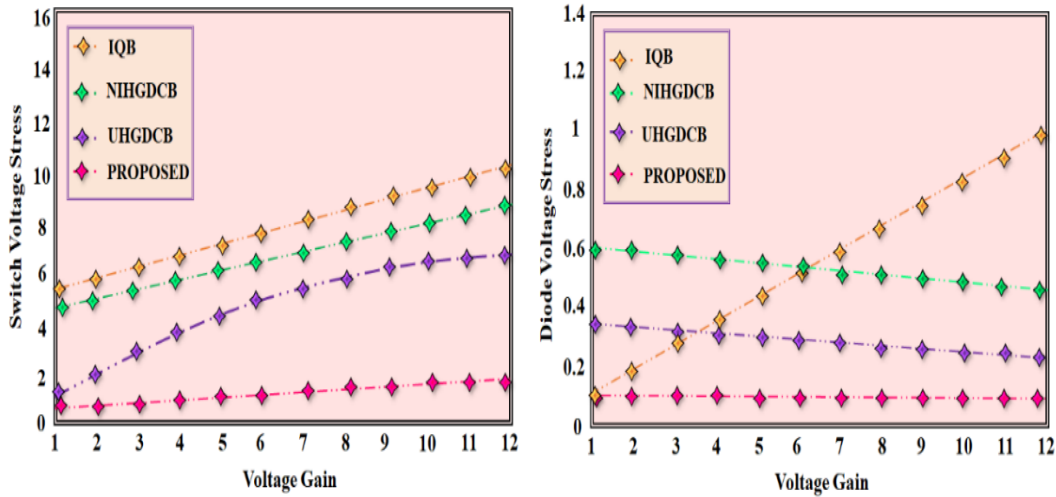
196

Fig. 20. Evaluation of Voltage Stress.

Voltage gain against duty cycle for IQB [11], NIHGDCB [13], UHGDCB [14], and the proposed converter compares in Fig. 19. As duty cycle approaches, the proposed converter shows a greater voltage gain of over than listed existing converters. This greater gain exhibits the proposed converter's capability to attain a greater voltage output at lower duty cycles, which extract more efficient operation.

Figure 20 illustrates switch and diode voltage stress as functions of voltage gain for four converters. The IQB, NIHGDCCB and UHGDCB converter shows the highest switch voltage stress as gain continues to increase. The proposed converter had the lowest switch stress, and most constant stress level across all gain levels, which is indicative of better stress management over the other converters. In the diode stress, the IQB, NIHGDCCB and UHGDCB converter had the highest diode voltage stress. The proposed converter consistently low diode voltage stress, improve durability for the converter, lower losses, and promote effective operation at higher gains.

Table 4.
Evaluation of Optimized PI controller performance.

Optimized PI Controller	Settling time (t_s)	Rise time (t_r)	Peak time (t_p)
PSO-GJ [21]	0.3912s	0.2197s	1.0546s
GWO [22]	0.518s	0.071s	0.812s
PROPOSED	0.07s	0.01s	0.03s

Table 4 comparative performance analysis of optimized PI controller such as PSO-Golden Jackal (GJ) [21], GWO [22] and proposed OOA-PI controller in terms of key dynamic response characteristics: (t_s), (t_s), and (t_s). The proposed controller outperformed the others listed controller with settling time of 0.07 s, rise time of 0.01 s, and peak time of 0.03 s.

V. CONCLUSION

This work presents an efficient PV energy conversion system with a CIS converter and an OOA-PI controller. With the help of CIS converter increasing the DC power produced by the PV panel even changing weather conditions. The design enables efficient transfer of energy with lower stress and high voltage gain, ensuring the highest efficiency of 96%. The OOA-PI controller achieves excellent performance by optimally tuning the PI gains for the controller to attain a very fast-responding system. The controller achieved a settling time of 0.07 s, a rise time of 0.01 s, and a peak time of 0.03 s with very little overshoot and stable under constant and changing load and reference conditions. The system modeled and validated in MATLAB/Simulink with the best accuracy through simulation of the converter behavior, controller dynamics, and real-time performance with different working conditions. The results of the proposed method ensure reliable, efficient, and high-quality power delivery for PV applications.

REFERENCES

[1] Yanarates, C. and Zhou, Z., Design and cascade PI controller-based robust model reference adaptive control of DC-DC boost converter. *IEEE access*, 2022, vol.10, pp. 44909-44922.

[2] Irshad, A. S., Elkholy, M. H., Alshammari, N. F., Ludin, G. A., Senjyu, T., Pinter, G. and Mikhaylov, A. Novel Approach for Energy Balancing with Intermittent Renewable Energy Source Using Multi-Objective Genetic Algorithm. *IEEE Access,* 2024.

[3] Priyadarshi, N., Padmanaban, S., Hiran, K. K., Holm-Nielsen, J. B., & Bansal, R. C. Artificial intelligence and Internet of things for renewable energy systems. *Artificial Intelligence and Internet of Things for Renewable Energy Systems*, 2021, vol. 12, 2021.

[4] Ali, C. B., Khan, A. H., Pervez, K., Awan, T. M., Noorwali, A. and Shah, S. A. High efficiency high gain DC-DC boost converter using PID controller for photovoltaic applications. *In 2021 International Congress of Advanced Technology and Engineering (ICOTEN)*, 2021, pp. 1-7.

[5] Arunkumar, G., Dhanamjayulu, C., Padmanaban, S., Prusty, B.R. and Khan, B. Implementation of optimization-based PI controller tuning for non-ideal differential boost inverter. *IEEE Access*, 2021, vol. 9, pp. 58677-58688.

[6] Inbamani, A. and Prabha, S. U. Predicting the Single Diode Model Parameters using Machine Learning Model. *Electric Power Components and Systems*, 2023, vol. 51, no. 14, pp. 1385-1397.

[7] Deželak, K., Bracinik, P., Sredenšek, K. and Seme, S. Proportional-integral controllers performance of a grid-connected solar PV system with particle swarm optimization and Ziegler–Nichols tuning method. *Energies*, 2021, vol. 14, no. 9, pp. 2516.

[8] Thirusenthil Kumaran, P., Vinayagam, A., Suganthi, S. T., Veerasamy, V., Inbamani, A., Chandran, J. and Farade, R. A. A voting approach of ensemble classifier for detection of power quality in islanded pv microgrid. *IETE Journal of Research*, 2023, vol. 69, no.10, pp. 7408-7424.

[9] Kavin, K. S., Karuvelam, P. S., Matcha, M. and Vendoti, S. Improved BRBFNN-based MPPT algorithm for coupled inductor KSK converter for sustainable PV system applications. *Electrical Engineering*, 2025, pp. 1-23.

[10] Kavin, K. S., Karuvelam, P. S., Kumar, R. T., Sivasubramanian, M., Kavitha, P., & Priyadharsini, S. GWO Optimized PI Controller Fed PV Based Interleaved Luo Converter for EV Applications. *In 2023 14th International Conference on Computing Communication and Networking Technologies (ICCCNT)*, 2023, pp. 1-6.

[11] Subhani, N., May, Z., Alam, M. K., Khan, I., Hossain, M. A. and Mamun, S. An improved non-isolated quadratic DC-DC boost converter with ultra high gain ability. *IEEE Access*, 2023, vol. 11 pp. 11350-11363.

[12] Abdel-Rahim, O. and Wang, H. A new high gain DC-DC converter with model-predictive-control based MPPT technique for photovoltaic systems. *CPSS Transactions on Power Electronics and Applications*, 2020, vol. 5, no. 2, pp. 191-200.

[13] Mahmood, A., Zaid, M., Ahmad, J., Khan, M. A., Khan, S., Sifat, Z. Alamri, B. A non-inverting high gain DC-DC converter with continuous input current. *IEEE access*, 2021, vol. 9, pp. 54710-54721.

[14] Khan, S., Zaid, M., Mahmood, A., Nooruddin, A. S., Ahmad, J., Alghaythi, M. L. and Lin, C. H. A new transformerless ultra high gain DC–DC converter for DC microgrid application. *IEEE Access*, 2021, vol. 9, pp. 124560-124582.

[15] Mohanta, H. C., Geetha, B. T., Alzaidi, M. S., Dhanoa, I. S., Bhambri, P., Mamodiya, U. and Akwafo, R. An Optimized PI Controller-Based SEPIC Converter for Microgrid-Interactive Hybrid Renewable Power Sources. *Wireless Communications and Mobile Computing*, 2022, no. 1, pp. 6574825.

[16] Roslan, M. F., Al-Shetwi, A. Q., Hannan, M. A., Ker, P. J. and Zuhdi, A. W. M. Particle swarm optimization algorithm-based PI inverter controller for a grid-connected PV system. *PloS one*, 2020, vol. 15, no. 12, pp. e0243581.

[17] Sivamani, D., Shyam, D., Ali, A. N., Premkumar, K., Narendiran, S. and Alexander, S. A. Solar powered battery charging system using optimized pi controller for buck boost converter. *In IOP Conference Series: Materials Science and Engineering*, 2021, vol. 1055, no. 1, pp. 012151.

[18] Vasumathi, G., Jayalakshmi, V. and Sakthivel, K. Efficiency analysis of grid tied PV system with KY integrated SEPIC converter. *Measurement: Sensors*, 2023, vol. 27, pp. 100767.

[19] Ellithy, H. H., Hasanien, H. M., Alharbi, M., Sobhy, M. A., Taha, A. M. and Attia, M. A. Marine predator algorithm-based optimal pi controllers for LVRT capability enhancement of grid-connected PV systems. *Biomimetics*, 2024, vol. 9, no. 2, pp. 66.

[20] Ibrahim, N. F., Alkuhayli, A., Beroual, A., Khaled, U. and Mahmoud, M. M. Enhancing the functionality of a grid-connected photovoltaic system in a distant Egyptian region using an optimized dynamic voltage restorer: Application of artificial rabbits optimization. *Sensor,* 2023, vol. 23, no. 16, pp. 7146.

[21] Arulselvan, K. and Padmanabhan, T. S. Adaptive Control Methods for Interacting Conical Tank Processes Using Optimization Algorithm. 2025.

[22] Negi, P., Pal, Y. and Gopinathan, L. Performance analysis of grid-connected photovoltaic systems using grey wolf optimisation and genetic algorithm. *International Journal of Power and Energy Conversion*, 2024, vol. 15, no. 2, pp. 122-146.

[23] Zhou, L.; Liu, X.; Tian, R.; Wang, W.; Jin, G. A Modified Osprey Optimization Algorithm for Solving Global Optimization and Engineering

Optimization Design Problems. *Symmetry* **2024**, *16*, 1173. https://doi.org/10.3390/sym16091173

[24] Zhang, Q.; Bu, X.; Zhan, Z.; Li, J.; Zhang, H. An efficient optimization state-based coyote optimization algorithm and its applications. Appl. Soft Comput. **2023**, 147, 110827.

Information about authors.

B. Kavya Santhoshi is working as Assistant Professor in the Department of Electrical & Electronics Engineering, School of Engineering, Godavari Global University, Rajahmundry. Her research interests include power electronics, renewable energy systems, and artificial intelligence applications in electrical engineering. Email: kavyasanthoshib@gmail.com
ORCID:0000-0002-5309-8159

R. V. L. N. S. Parvathi is working in Godavari Institute of Engineering and Technology affiliated from Jawaharlal Nehru Technological University, Kakinada. Her main area of interest includes, Power Electronics and renewable energy systems. Email: parvathi4314@gmail.com
ORCID: 0000-0002-6633-9897

Gudiguntla Harshith Tharpil present studying in department of Electrical and Electronics Engineering in Godavari Institute of Engineering and Technology affiliated from Jawaharlal Nehru Technological University, Kakinada. His research interests include power electronics, renewable energy systems,
Email:
 gharshithtarpil@gmail.com

Murapaka Krishna Vamsi present studying in department of Electrical and Electronics Engineering in Godavari Institute of Engineering and Technology affiliated from Jawaharlal Nehru Technological University, Kakinada. His research interests include power electronics, renewable energy systems.
Email:
murapakakrishna18@gmail.com

Kumara Manohar Appaji present studying in department of Electrical and Electronics Engineering in Godavari Institute of Engineering and Technology affiliated from Jawaharlal Nehru Technological University, Kakinada. His research interests include power electronics, renewable energy systems,
Email:
manoharkumara32408@gmail.com